Spatio-temporal dynamics through standardized CPUE for blue shark caught by the Taiwanese large-scale tuna longline fishery in the Indian Ocean from 2005 to 2023

Hoang Huy Huynh^{1,2,3} and Wen-Pei Tsai^{1,2,*}

^{*} Corresponding author. E-mail: wptsai@nkust.edu.tw (W.-P. Tsai).



¹ Chondrichthyan Resources Sustainability Research Center, National Kaohsiung University of Science and Technology, Kaohsiung 81157, Taiwan

² Department of Fisheries Technology and Management, National Kaohsiung University of Science and Technology, Kaohsiung 81157, Taiwan

³ Institute of Aquatic Science and Technology, National Kaohsiung University of Science and Technology, Kaohsiung 81157, Taiwan

ABSTRACT

Understanding spatiotemporal variability is crucial for accurate stock assessments and effective fishery management. This study examines the relative abundance of blue sharks (*Prionace glauca*) in the Indian Ocean using observer-based catch per unit effort (CPUE) data from the Taiwanese large-scale longline fishery collected between 2005 and 2023. We applied a spatiotemporal modeling approach (sdmTMB) to standardize the CPUE index. The nominal CPUE series displayed significant interannual variability, particularly a sharp decline in 2015. In contrast, the standardized CPUE exhibited a clearer trend: it increased steadily from 2005 to 2013, then fluctuated moderately but remained relatively stable through 2023. The coefficient of variation of standardized estimates decreased significantly from 28.0% to 12.0% during 2005–2013, indicating enhanced model precision, and stayed consistently below 25% thereafter. Spatial analyses identified recurring hotspots of blue shark abundance in the southwestern and southeastern Indian Ocean, especially during specific years and quarters, along with notable seasonal and interannual shifts in distribution. These findings highlight the importance of spatiotemporal standardization and suggest that blue shark abundance has remained relatively stable over the past two decades, potentially indicating optimal utilization. Future assessments should integrate environmental covariates to improve inference and support ecosystem-based management.

Keywords: blue shark; CPUE standardization; Indian Ocean; sdmTMB model; sustainable shark fishing; spatiotemporal model.

1. Introduction

The blue shark (*Prionace glauca*) is a resilient pelagic species often caught as bycatch in longline fisheries targeting tuna (*Thunnus* spp.) and swordfish (*Xiphias gladius*) (Aires-da-Silva and Gallucci, 2007; Coelho et al., 2012). Global annual mortality is estimated at 10.74 million individuals (Clarke et al., 2006). In the Indian Ocean, the blue shark coexists with at least ten other shark bycatch species, yet it makes up only 2.0% of the overall bycatch composition (Huang, 2011). It is currently listed as Near Threatened by the IUCN (Rigby et al., 2019). Despite its ecological significance (Lucrezi et al., 2024), assessments often focus heavily on landings from industrial fleets, neglecting discards and unreported catches. This oversight undermines effective ecosystem-based management (Huang, 2011; Lascelles et al., 2014).

Uncertainty in stock assessments remains high due to underreporting; only 72% of catches were reported in 2019 (IOTC, 2019), which has resulted in an underestimation of fishing mortality (IOTC, 2021). Catch-per-unit-effort (CPUE) is a commonly used proxy for relative abundance, but its reliability depends on rigorous standardization to reduce biases in fisheries-dependent data (Ducharme-Barth et al., 2022; Hoyle et al., 2024). Recent advances in spatiotemporal modeling, particularly the use of generalized linear mixed models (GLMMs) (Thorson, 2019; Grüss et al., 2023), have greatly enhanced stock assessments by capturing spatial heterogeneity and temporal dynamics. Notably, the sdmTMB framework accounts for both spatial autocorrelation and temporal variation by integrating spatial random fields and time-varying effects (Anderson et al., 2024). This modeling approach enables more realistic inference from fisheries-dependent data by capturing distributional shifts and spatial heterogeneity, which are critical for interpreting changes in blue shark abundance over time.

This working paper expands on earlier research that utilized a delta-lognormal model to estimate standardized CPUE for blue sharks from 2005 to 2020 (IOTC–2022–WPEB18-19). In this study, we extend the analysis to include data up to 2023 and implement the sdmTMB framework, which allows us to incorporate spatial and temporal correlation structures. This enhanced approach provides a more thorough investigation of blue shark distribution dynamics in the Indian Ocean, offering valuable insights for regional stock assessments and conservation planning.

2. Materials and methods

2.1. Fisheries observer data

Catch and effort data for blue sharks (BSH) were collected from scientific observers on Taiwanese large-scale longline vessels, coordinated by the Overseas Fisheries Development Council of Taiwan, from 2005 to 2023. This dataset includes comprehensive records of catch quantities, the number of hooks deployed, and spatiotemporal coordinates (date, latitude, longitude) for each fishing operation. The analysis also incorporates additional variables such as hooks, hooks per basket (HPB), and vessel size (CTNO).

2.3. Filtering and exploration of data

Prior to standardization, records lacking essential information (e.g., latitude, longitude, hooks, or HPB) were excluded. Between 2005 and 2023, the filtered dataset comprised 78,244,649 hooks and 56,584 blue sharks (BSH), forming the basis for CPUE analyses (annual trends shown in **Fig. 1**). Nominal CPUE (nCPUE), calculated as the number of BSH caught per 1,000 hooks, ranged from 0 to 49.3, with a mean of 0.73 and a standard deviation of 1.77. Notably, 53.7% of the observations recorded a value of zero. The data exhibited a high degree of right skewness (skewness = 9.53) and overdispersion, indicative of the infrequent nature of catch events. The Anderson–Darling test strongly rejected the assumption of normality (A = 5127.8; $p < 2.2 \times 10^{-16}$; Anderson and Darling, 1954). Given the zero inflation, skewness, and discreteness of the data, a tailored CPUE standardization approach was required to obtain reliable abundance indices.

2.3. CPUE standardization statistical modeling

To standardize nCPUE while accounting for variable fishing effort and spatiotemporal dependencies, we applied a spatiotemporal generalized linear mixed model (GLMM) using the sdmTMB framework. This approach enhances traditional GLMMs by integrating spatial and spatiotemporal structures through Gaussian Random Fields (GRFs). In this way, fisheries data can be used to estimate abundance indices better (Anderson et al., 2024). The expected catch per set $\mu_i = E[BSH_i]$ was modeled as:

$$\log(\mu_i) = X_i \beta + \omega(s_i) + \varepsilon(s_i, t_i) + \log(effort_i),$$

where $X_i\beta$ represents the fixed effects; $\omega(s_i)$ is the spatial random effect modeled using a GRFs; and $\varepsilon(s_i,t_i)$ is the spatiotemporal random effect following an AR(1) process at each location s_i : $\varepsilon(s_i,t_i) = \rho\varepsilon(s_i,t_{i-1}) + \eta(s_i,t_{i-1})$ with ρ : temporal autocorrelation coefficient (-1 < p < 1); $\eta(s_i,t_i) \sim N(0,\sigma_\varepsilon^2)$ normally distributed innovations.; $\log(effort_i)$: offset term (number of hooks used). Fishing effort was standardized by including the log-transformed number of hooks per set as an offset term. A spatial mesh with 212 knots was constructed (Fig. 2) to balance spatial resolution and computational efficiency.

The explanatory variables included: Year (2005–2023); Quarter Q1 (January–March), Q2 (April–June), Q3 (July–September), and Q4 (October–December); gear configuration (HPBC), categorized as shallow (<5 HPB), middle (5–10), deep (10–15), and ultra-deep (≥15); and CTNO, classified into CT5, CT6, and CT7.

2.4. Models selection

Model selection was conducted in two stages. In the first stage, several observation families: Poisson, Negative Binomial 1 (NB1, linear), Negative Binomial 2 (NB2, quadratic), Tweedie, delta-gamma, and delta-lognormal - were assessed using a full fixed-effects structure to ensure comparability. The best-performing family was identified based on the Akaike Information Criterion (AIC; Akaike, 1973) and Bayesian Information Criterion (BIC; Schwarz, 1978). In

the second stage, the fixed-effects structure was refined using the chosen family. Candidate variables were iteratively added or removed, with model selection guided by statistical significance and information-theoretic criteria, including AIC, BIC, and Akaike weights, to optimize the balance between model fit and complexity.

Model adequacy was evaluated using residual diagnostics from the sdmTMB framework. This included Q–Q (quantile-quantile) plots and dispersion tests utilizing the DHARMa package, along with annual Q–Q plots to assess temporal consistency. Spatial autocorrelation was analyzed using Moran's I, and residual maps were reviewed to identify potential spatial biases.

2.5. Estimation of standardized CPUE and uncertainty

Standardized CPUE trends and associated uncertainty were estimated using the best-performing sdmTMB model. We conducted posterior simulations to generate CPUE predictions and derived 95% confidence intervals using a bias-corrected percentile method. To facilitate year-to-year comparisons, all standardized CPUE values were normalized to their overall mean. This approach enhances the clarity of trends and highlights differences between nominal and standardized indices while accounting for variations in sampling effort.

The coefficient of variation (CV) for each year's CPUE was calculated as the ratio of the standard error to the mean, providing a relative measure of uncertainty across years. All analyses and visualizations were performed in R (v4.4.2) using the sdmTMB package (Anderson et al., 2024; github.com/pbs-assess/sdmTMB).

3. Results and discussion

3.1. Selection of the best model

All candidate families successfully converged (maximum gradient < 0.0001), with the delta-lognormal model (M-6) providing the best fit according to AIC and BIC (**Table 1**). Using this family, we tested multiple sdmTMB models, among which Model M-5 demonstrated the strongest support, indicated by the lowest AIC and BIC values and an Akaike weight of 1.00. All models in this set, except for the NULL model (gradient = 0.0019), also converged well (**Table 2**). Consequently, Model M-5 was chosen for further analysis.

The adequacy of Model M-5 was confirmed through diagnostic checks (**Figs. 3–6**). Residual plots (**Fig. 3**) indicated no significant deviation from uniformity (*KS* test, p = 0.536), although overdispersion and outliers were significant (both p < 0.001). No spatial autocorrelation was found (Moran's I = 0.004, p = 0.16; **Fig. 4**), and temporal Q-Q plots, along with spatiotemporal residuals (**Figs. 5–6**), revealed no major deviations or clustering.

3.2. The trends of CPUE

The nominal CPUE series exhibited significant interannual variability, particularly with a marked decline in 2015. In contrast, the standardized CPUE estimates from the sdmTMB model indicated a clearer trend, showing a steady increase from 2005 to 2013, followed by moderate fluctuations. During the period from 2005 to 2013, the CV decreased significantly from 28.0% to 12.0%, representing a 57.1% reduction and demonstrating notable improvements in model precision. Although some interannual variability continued after 2013, all CV values remained below 25%, suggesting a stable and reliable phase for abundance estimation. These findings indicate that blue shark abundance in the Indian Ocean has remained relatively stable, with potential signs of optimal utilization between 2005 and 2023 (Table 3; Fig. 7).

3.3. Spatiotemporal dynamics

The spatial distribution of standardized CPUE for blue sharks ranged from 10°S to 45°S, featuring two high-abundance cores: (1) the southwestern region (20°E–40°E) and (2) the southeastern region (80°E–110°E), both concentrated around 30°S to 45°S. Moderate abundance was observed patchily across central longitudes (50°E–80°E) (**Fig. 8**). Quarterly patterns revealed dynamic shifts in blue shark distribution, with higher CPUE noted in the southeastern Indian Ocean during Quarter 1, while other quarters displayed varying hotspots (**Fig. 9**). Interannual variability in blue shark CPUE from 2005 to 2023 indicated intermittent hotspots in the southwestern Indian Ocean, alongside low abundance in northern areas (**Fig. 10**). Notably, hotspots were present in both the southwestern and southeastern regions in 2009. After 2015, spatial coverage expanded, resulting in widespread moderate-to-high CPUE.

This paper highlights the effectiveness of spatiotemporal modeling in analyzing the distribution and relative abundance of blue sharks in the Indian Ocean (Grüss et al., 2019; Fuster-Alonso et al., 2024; Hoyle et al., 2024). The findings indicate quarterly and interannual variations in CPUE, which reflect the species' extensive mobility and habitat utilization. These variations are likely influenced by changing oceanographic conditions, prey availability, and fishing effort. Although environmental variables were not included in the model, it still provides valuable insights into spatiotemporal trends.

Despite its contributions, the study has limitations, such as the lack of fishery-independent data and incomplete spatial coverage. Future research should incorporate environmental covariates, extend the observer data series, and consider size- or sex-specific habitat use to enhance stock assessments and spatial management.

Overall, this working paper supports the application of spatiotemporal standardization in data-limited contexts and advocates for utilizing predicted CPUE from Taiwanese longline fisheries as a reliable abundance index for blue sharks in the Indian Ocean.

References

- Aires-da-Silva, A.M. and Gallucci, V.F., 2007. Demographic and risk analyses applied to management and conservation of the blue shark (Prionace glauca) in the North Atlantic Ocean. Marine and Freshwater Research, 58(6), pp.570-580.
- Akaike, H., 1973. Information theory and an extension of maximum likelihood principle, pp. 267-281.
- Anderson, S.C., Ward, E.J., English, P.A. and Barnett, L.A. 2024. sdmTMB: an R package for fast, flexible, and user-friendly generalized linear mixed effects models with spatial and spatiotemporal random fields. BioRxiv, 2022.2003. 2024.485545.
- Anderson, T. W., Darling, D. A., 1954. A Test of Goodness of Fit. Journal of American Statistical Association, 49, 765-769.
- Clarke, S.C., McAllister, M.K., Milner-Gulland, E.J., Kirkwood, G.P., Michielsens, C.G., Agnew, D.J., Pikitch, E.K., Nakano, H. and Shivji, M.S., 2006. Global estimates of shark catches using trade records from commercial markets. Ecology letters, 9(10), pp.1115-1126.
- Coelho, R., Fernandez-Carvalho, J., Lino, P.G. and Santos, M.N., 2012. An overview of the hooking mortality of elasmobranchs caught in a swordfish pelagic longline fishery in the Atlantic Ocean. Aquatic Living Resources, 25(4), pp.311-319.
- Ducharme-Barth, N.D., Grüss, A., Vincent, M.T., Kiyofuji, H., Aoki, Y., Pilling, G., Hampton, J. and Thorson, J.T., 2022. Impacts of fisheries-dependent spatial sampling patterns on catch-per-unit-effort standardization: a simulation study and fishery application. Fisheries Research, 246, p.106169.
- Fuster-Alonso, A., Conesa, D., Cousido-Rocha, M., Izquierdo, F., Paradinas, I., Cerviño, S., Pennino, M. G., 2024. Accounting for spatio-temporal and sampling dependence in survey and CPUE biomass indices: simulation and Bayesian modeling framework. ICES Journal of Marine Science 81(5), 984-995.
- Grüss, A., McKenzie, J.R., Lindegren, M., Bian, R., Hoyle, S.D. and Devine, J.A., 2023. Supporting a stock assessment with spatio-temporal models fitted to fisheries-dependent data. Fisheries Research, 262, p.106649.
- Grüss, A., Walter III, J.F., Babcock, E.A., Forrestal, F.C., Thorson, J.T., Lauretta, M.V. and Schirripa, M.J., 2019. Evaluation of the impacts of different treatments of spatio-temporal variation in catch-per-unit-effort standardization models. Fisheries Research, 213, pp.75-93.
- Hoyle, S. D., Campbell, R. A., Ducharme-Barth, N. D., Grüss, A., Moore, B. R., Thorson, J. T., Tremblay-Boyer, L., Winker, H., Zhou, S., Maunder, M. N., 2024. Catch per unit effort modelling for stock assessment: A summary of good practices. Fisheries Research 269, 106860.
- Hoyle, S.D., Campbell, R.A., Ducharme-Barth, N.D., Grüss, A., Moore, B.R., Thorson, J.T., Tremblay-Boyer, L., Winker, H., Zhou, S. and Maunder, M.N., 2024. Catch per unit effort modelling for stock assessment: A summary of good practices. Fisheries Research, 269, p.106860.
- Huang, H.W., 2011. Bycatch of high sea longline fisheries and measures taken by Taiwan: Actions and challenges. Marine Policy, 35(5), pp.712-720.
- IOTC., 2019. Report on IOTC data collection and statistics. Mahé, Seychelles: IOTC Secretariat.
- IOTC., 2021. Review of the statistical data available for bycatch species Mahé, Seychelles: Indian Ocean Tuna Commission.
- Lascelles, B., Notarbartolo Di Sciara, G., Agardy, T., Cuttelod, A., Eckert, S., Glowka, L., Hoyt, E., Llewellyn, F., Louzao, M., Ridoux, V. and Tetley, M.J., 2014. Migratory marine species: their status, threats and conservation management needs. Aquatic Conservation: Marine and Freshwater Ecosystems, 24(S2), pp.111-127.
- Lucrezi, S. and Matiza, T., 2024. Sharks, tourism and conservation: a test of causative and mediating effects on scuba divers' attitude. Marine Policy, 160, p.105996.
- Rigby, C.L., Barreto, R., Carlson, J., et al., 2019. Prionace glauca. IUCN Red. List Threat Species. https://doi.org/10.2305/IUCN.UK.2019-3.RLTS.T39381A2915850.en.
- Schwarz, G., 1978. Estimating the dimension of a model. The annals of statistics, pp.461-464.
- Thorson, J.T., 2019. Guidance for decisions using the Vector Autoregressive Spatio-Temporal (VAST) package in stock, ecosystem, habitat and climate assessments. Fisheries Research, 210(February), pp.143-161.

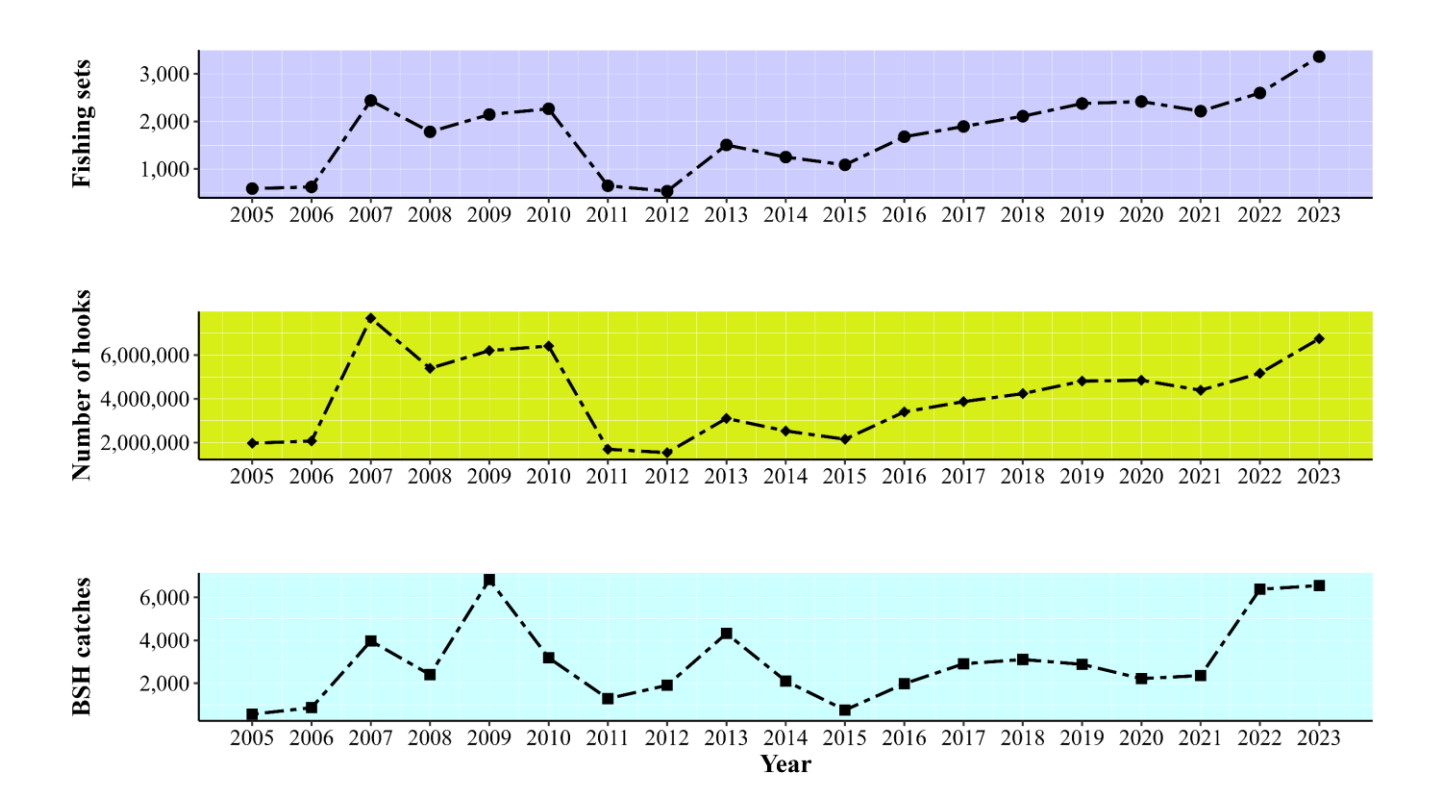


Fig. 1. Annual summary of observer data for BSH, including longline fishing sets, the number of hooks used, and the total BSH catch (in numbers).

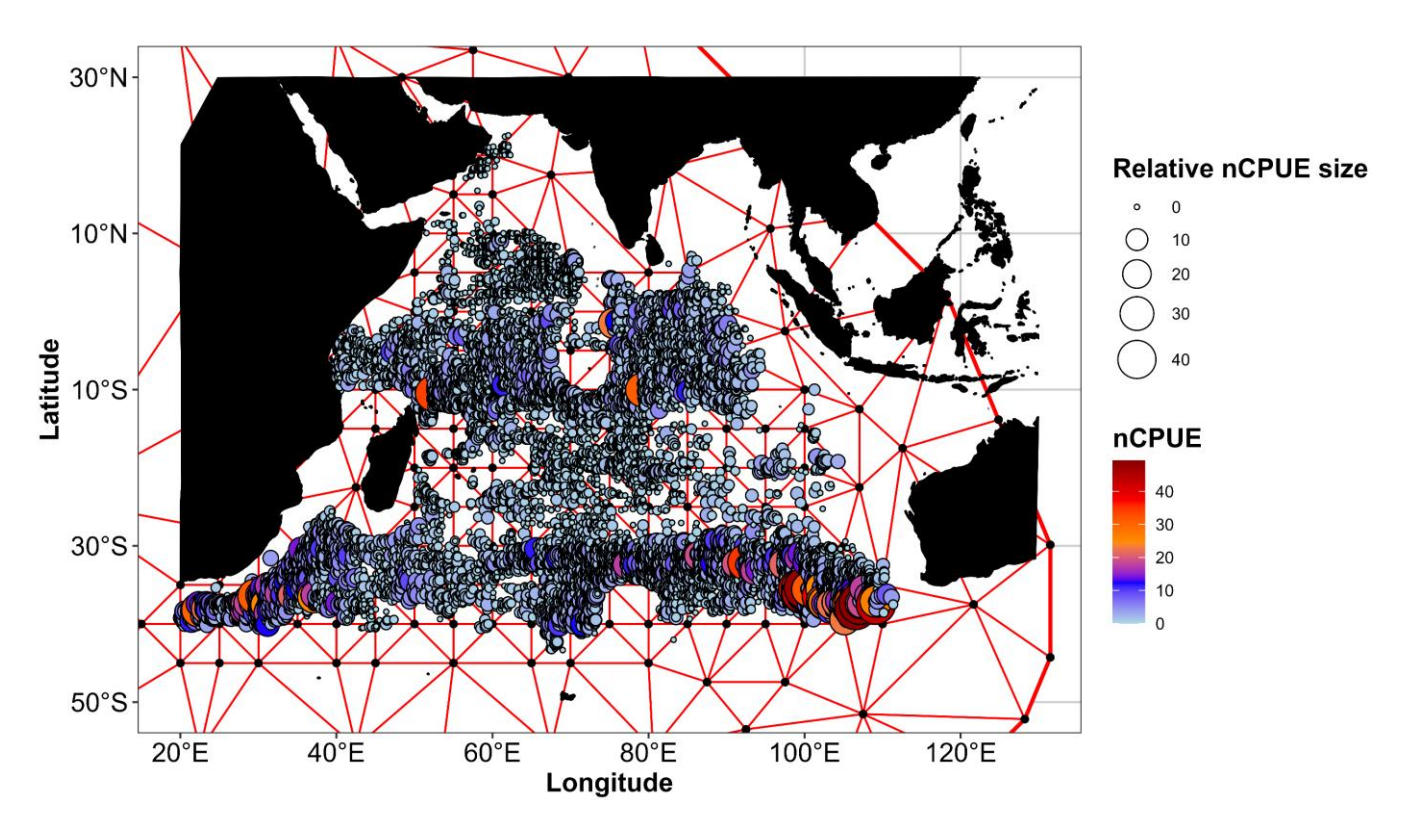


Fig. 2. Mesh structure and observed nominal CPUE values for sdmTMB modeling. Each circle represents a fishing set location, with size and color indicating relative nominal CPUE.

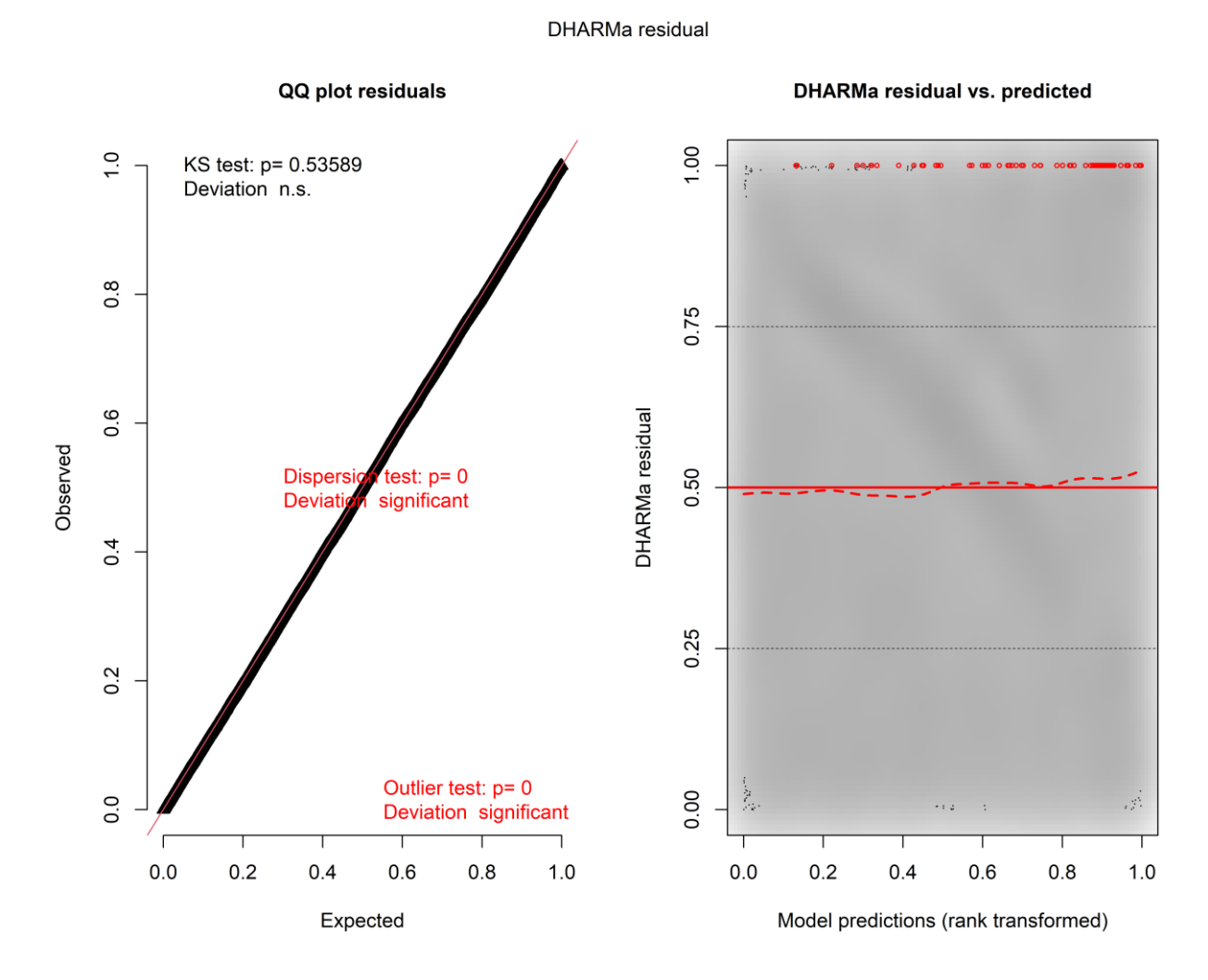


Fig. 3. Residual diagnostics for sdmTMB model using DHARMa.

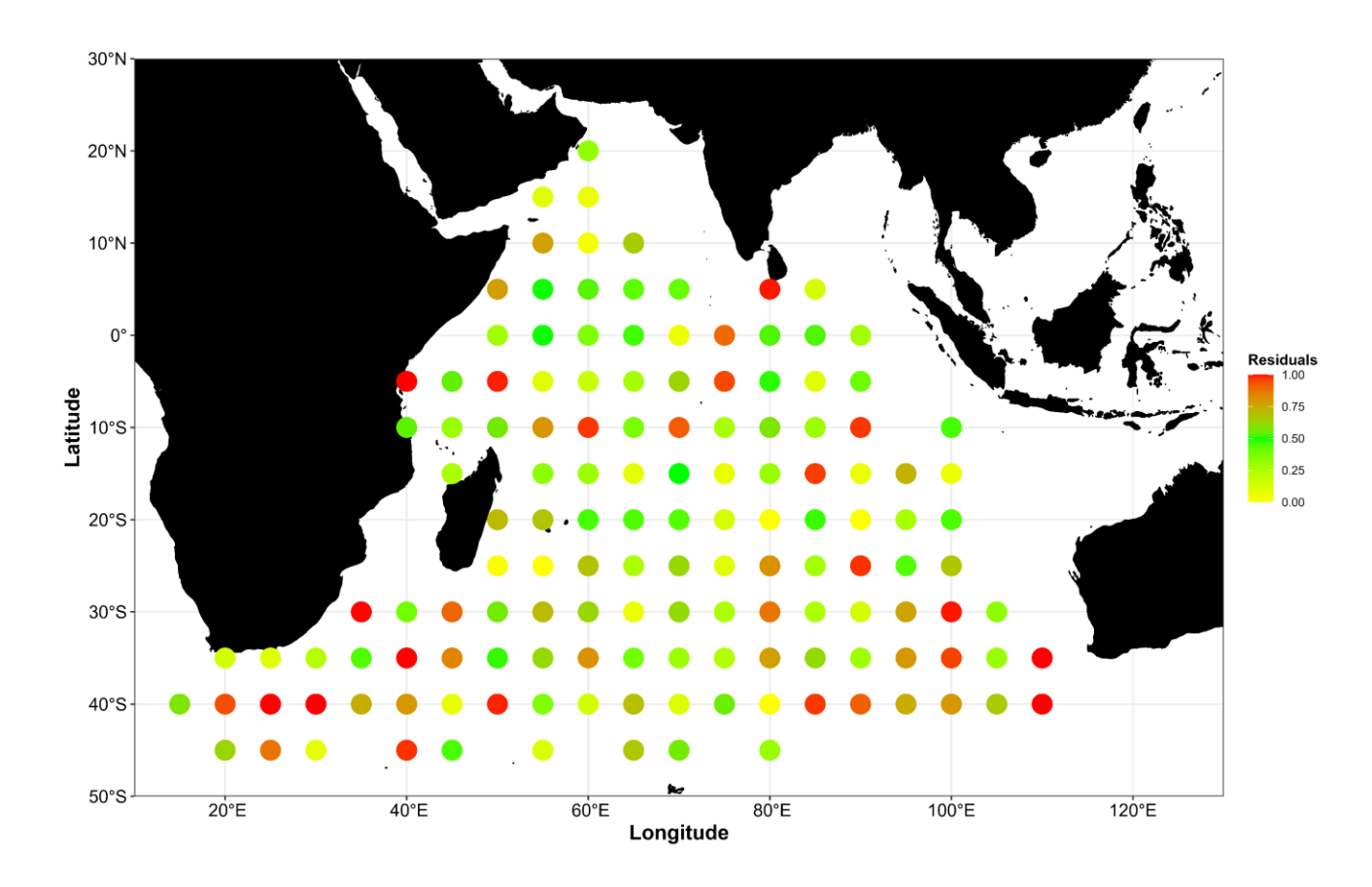


Fig. 4. Residual diagnostics for sdmTMB model: Spatial residual patterns with Moran's I test results.

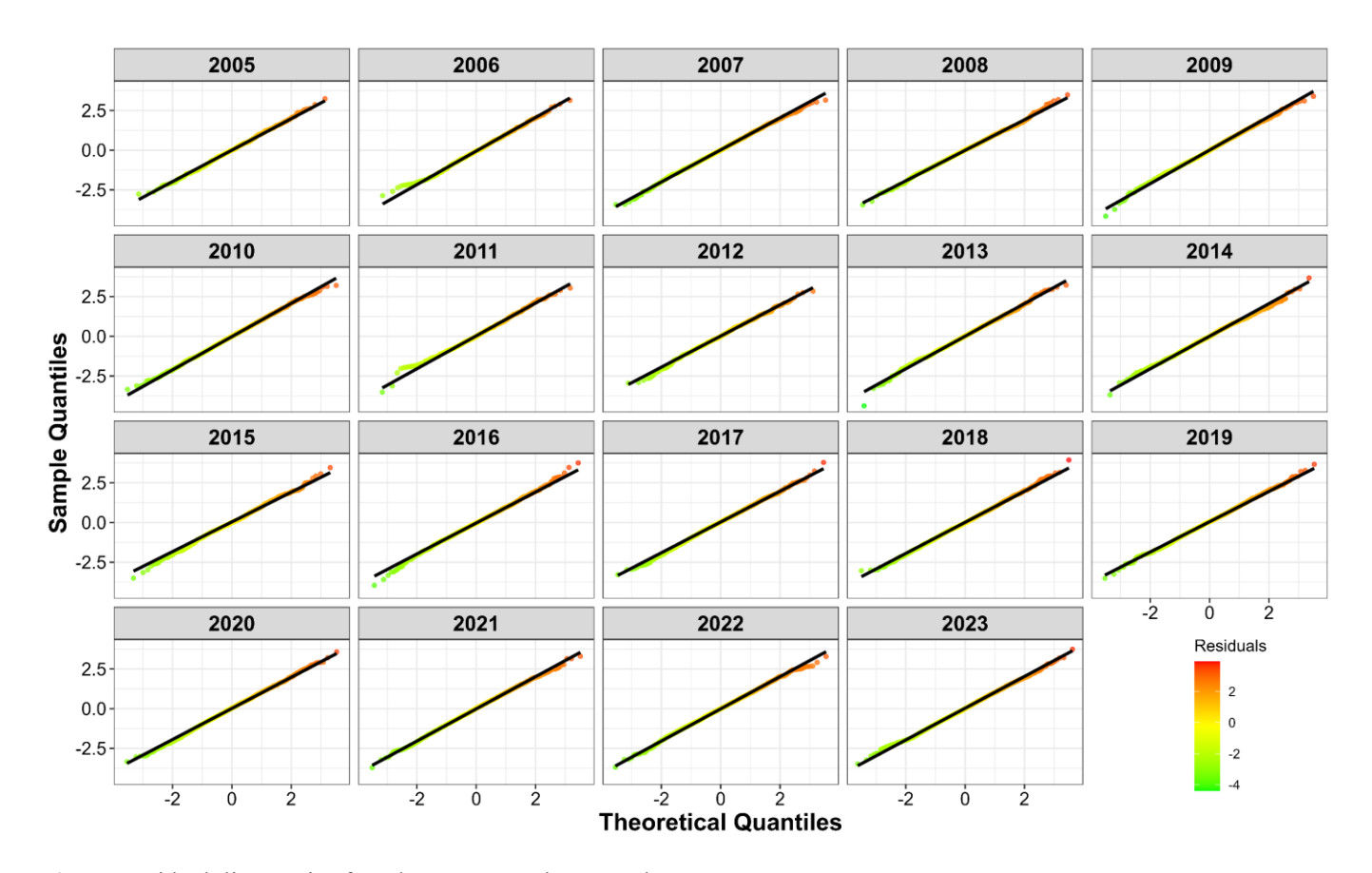


Fig. 5. Residual diagnostics for sdmTMB: Yearly Q-Q plots.

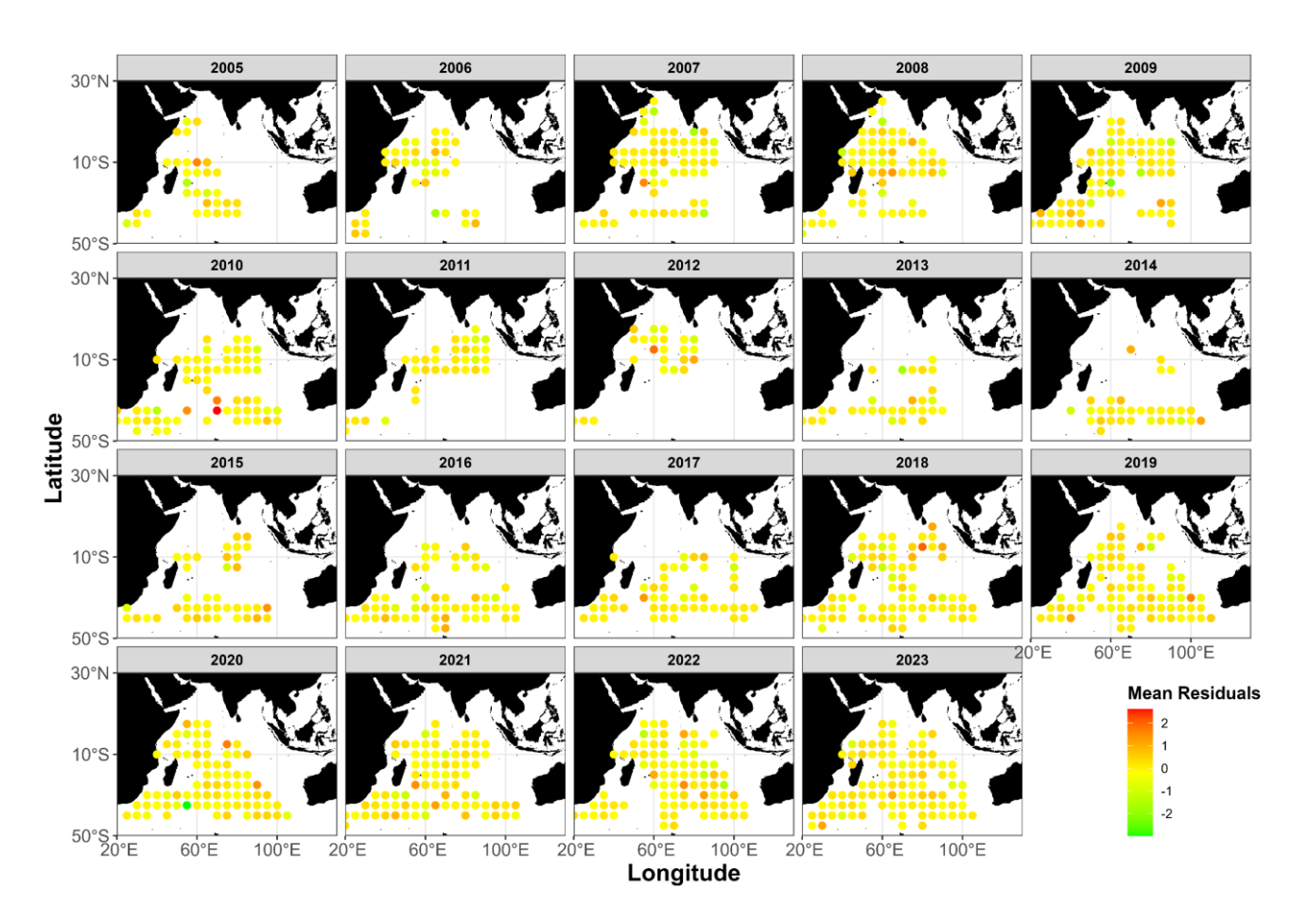


Fig. 6. Residual diagnostics for sdmTMB: Spatiotemporal residual distributions by year.

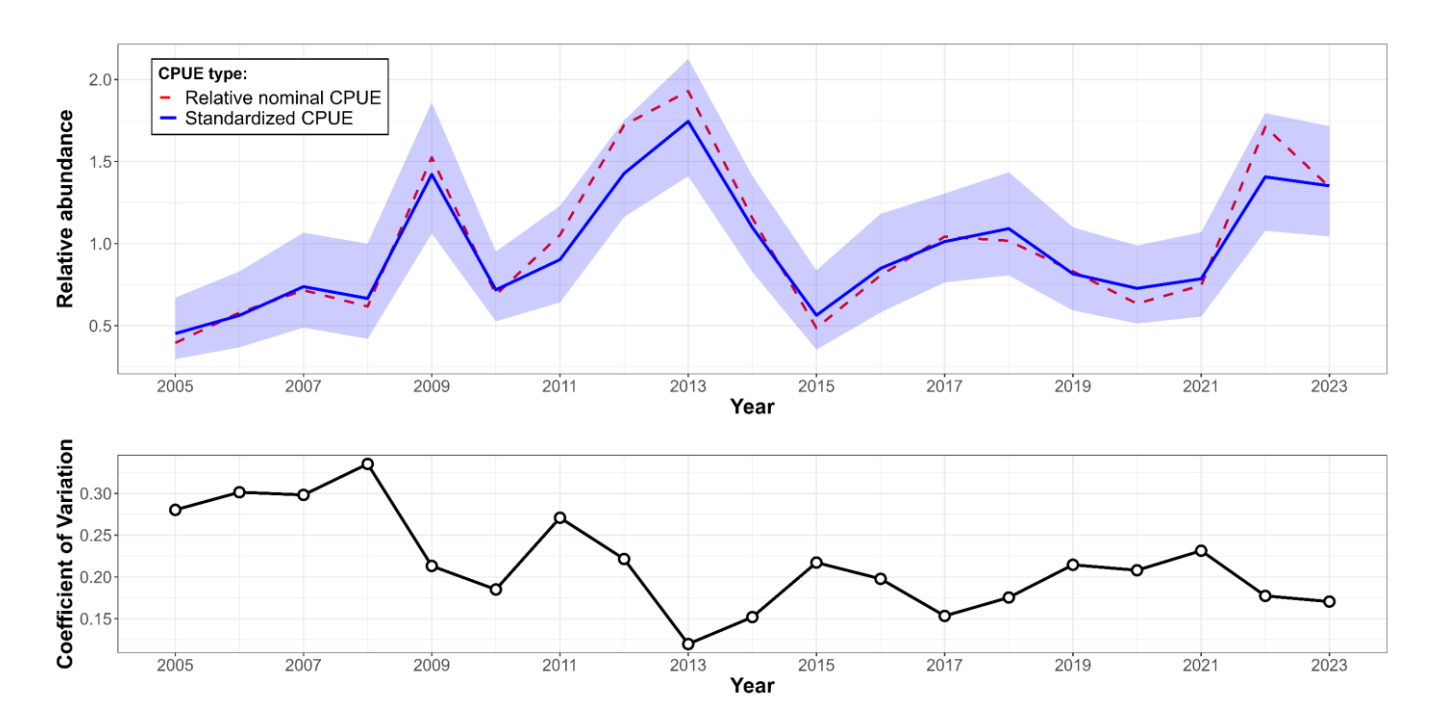


Fig. 7. Top: Time series of nominal and standardized CPUE estimates for blue sharks in the Indian Ocean (2005–2023), derived from sdmTMB models. Shaded areas represent 95% confidence intervals. Bottom: Coefficient of variation (CV) for the standardized abundance indices.

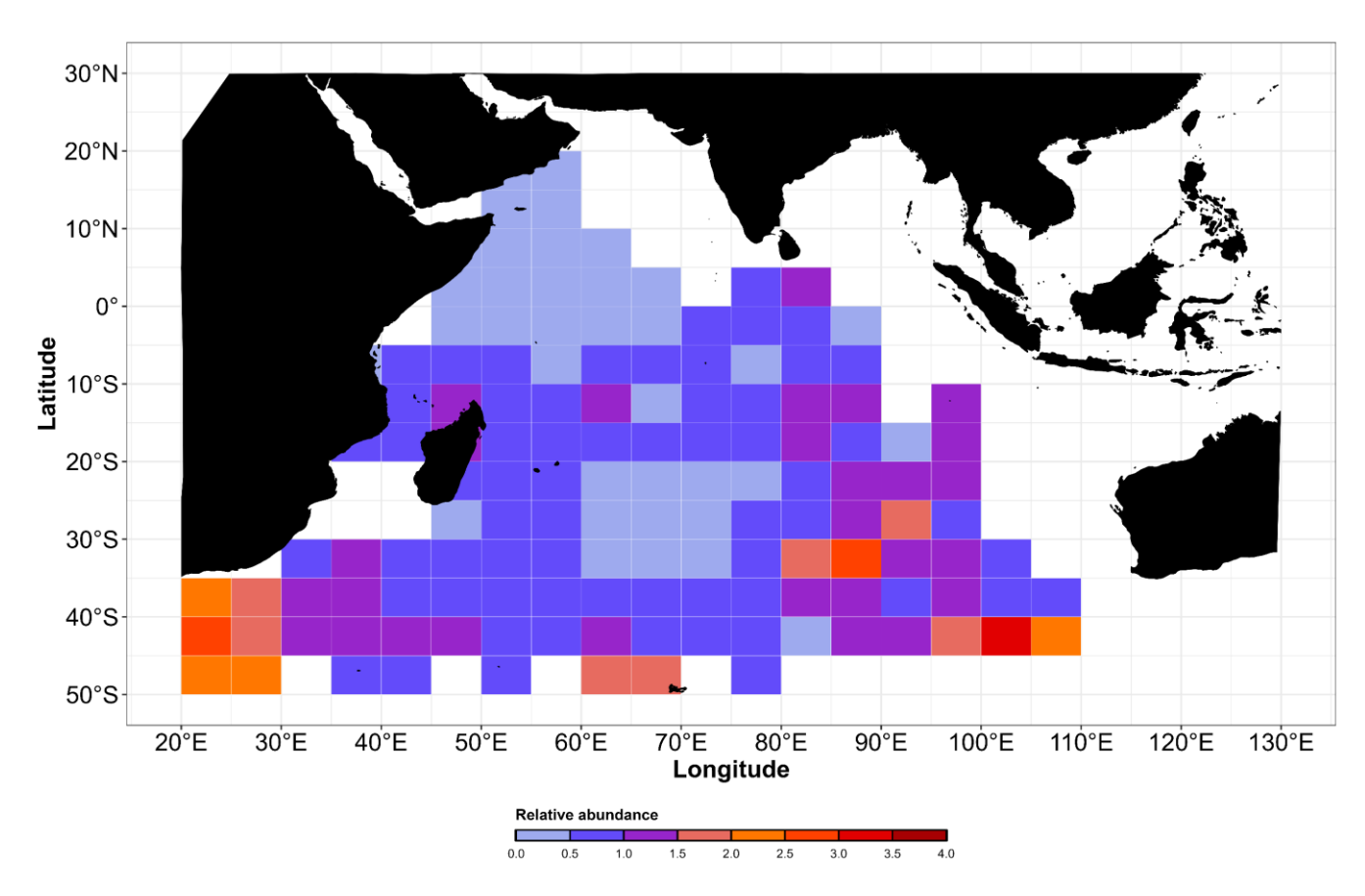


Fig. 8. Spatial distribution of standardized CPUE for blue sharks in the Indian Ocean, using aggregated data from 2005 to 2023.

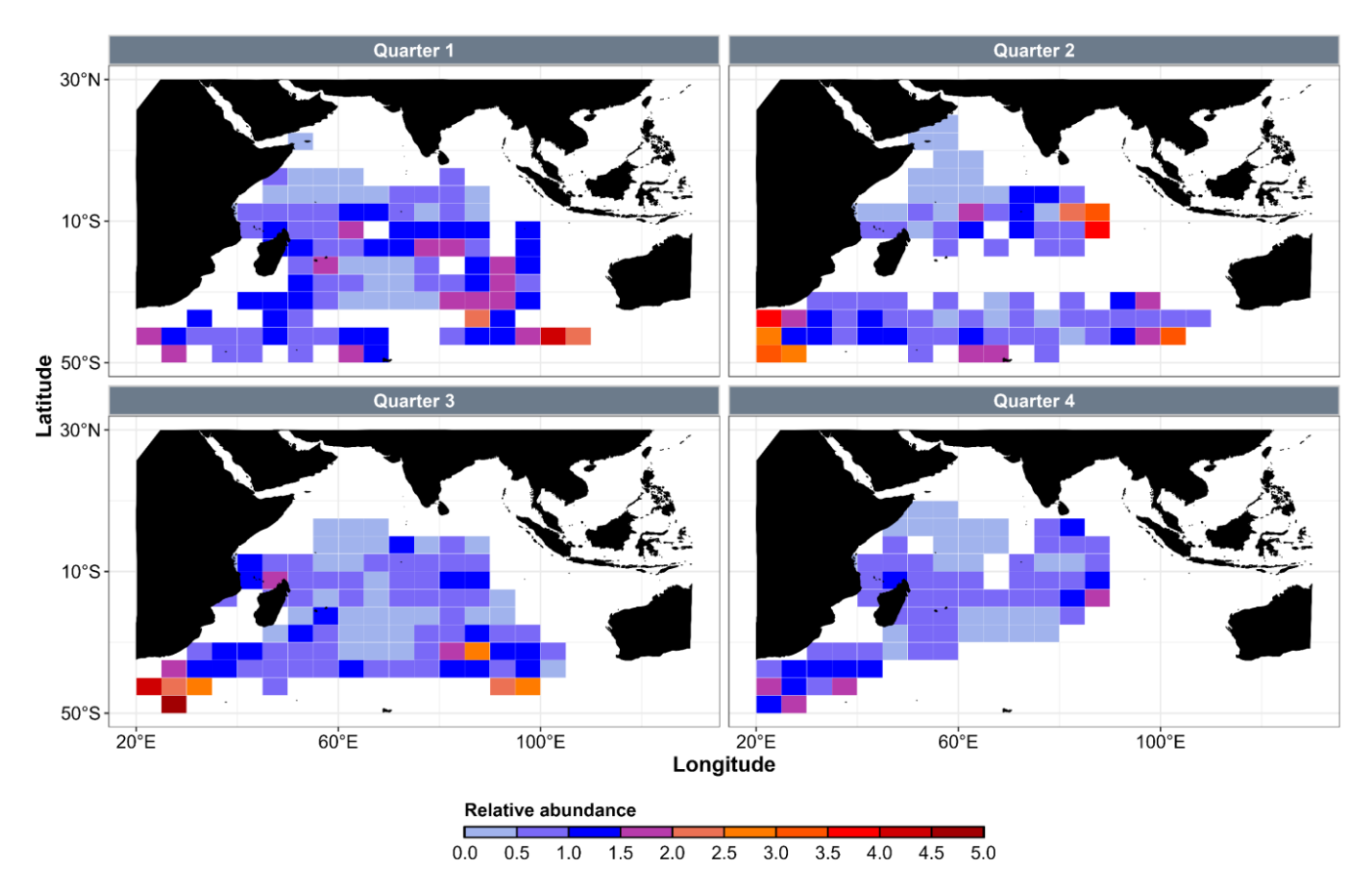


Fig. 9. Distribution of the standardized CPUE for blue sharks in the Indian Ocean over the period of 2005 to 2023 by quarterly patterns.

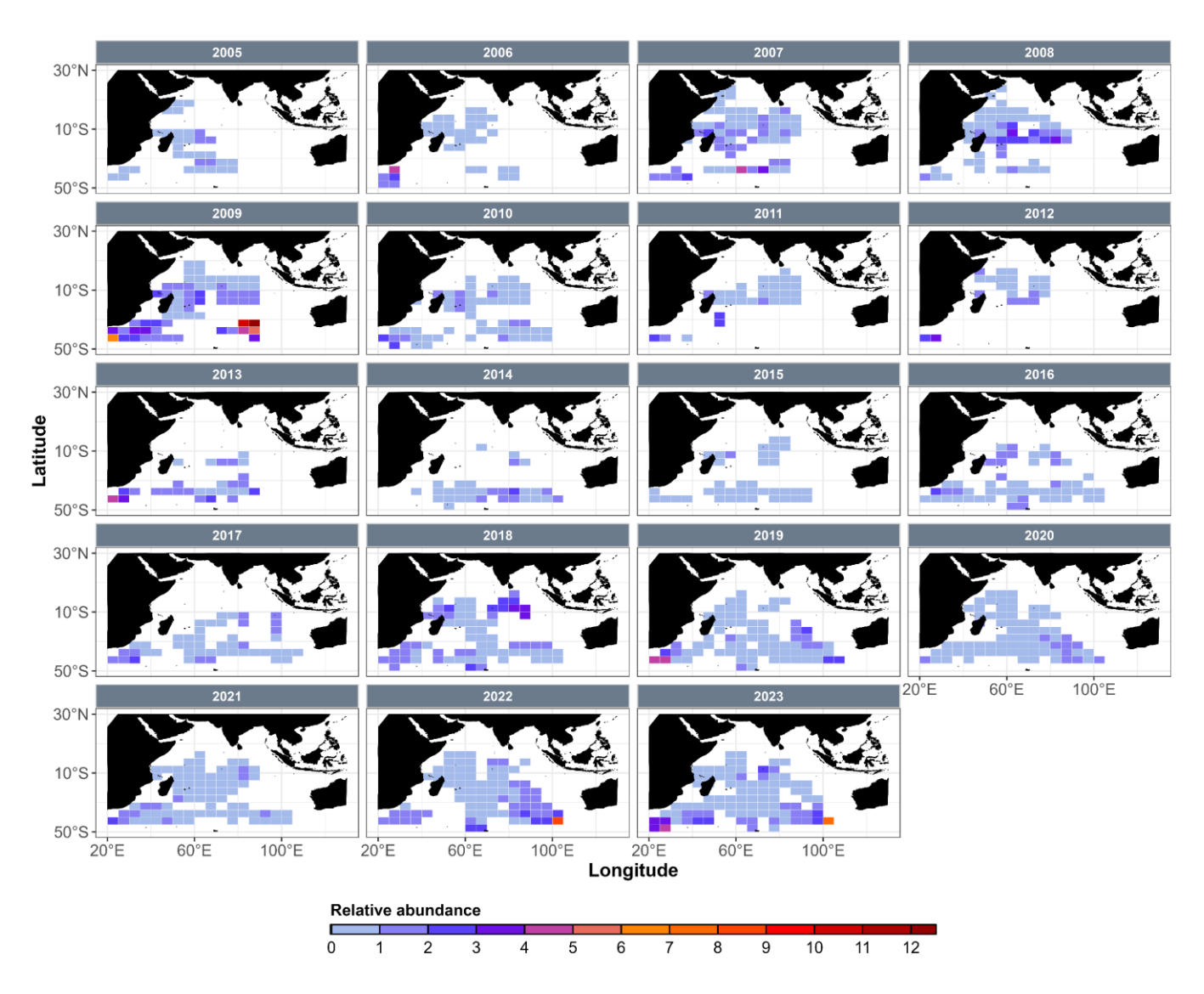


Fig. 10. Annual spatiotemporal distribution of standardized CPUE for blue sharks in the Indian Ocean from 2005 to 2023.

Table 1. Comparison of alternative observation model families for blue shark CPUE in the Indian Ocean, using a full fixed-effects structure. The table reports the number of parameters, AIC, Δ AIC, BIC, Δ BIC, and maximum gradient. " Δ " indicates the difference from the minimum value. The best-performing model (bolded) was selected for further refinement.

Model	Model type	No. parameters	AIC	ΔΑΙС	BIC	ΔΒΙC	Maximum gradient
M-1	Tweedie	37	103649.1	4765.1	103800.7	4638.8	< 0.0001
M-2	Poisson	35	133275.8	34391.8	133410.5	34248.6	< 0.0001
M-3	Delta-gamma	52	101076.4	2192.4	101354.3	2192.4	< 0.0001
M-4	Negative Binomial 1 (linear)	36	101882.4	2998.4	102025.6	2863.7	< 0.0001
M-5	Negative Binomial 2 (quadratic)	36	100711.3	1827.3	100854.4	1692.6	< 0.0001
M-6	Delta-lognormal	52	98884.0	0.0	99161.9	0.0	< 0.0001

Table 2. Comparison of fixed-effects structures using the delta-lognormal model (sdmTMB) for blue shark CPUE. Metrics include the number of parameters (No. pa), residual degrees of freedom (Res. DF), AIC, Δ AIC, BIC, Δ BIC, Akaike weight, and maximum gradient. "Station" represents spatial (latitude and longitude) effects. The NULL model includes only the intercept. The best-fitting model (bolded) was selected for further analysis..

Model	Model structure	No. pa	Res. DF	AIC	ΔΑΙС	BIC	ΔΒΙС	Akaike weight	Maximun gradient
M-1	NULL	22	33509	110370.4	11486.4	110395.7	11233.81	0.00	0.0019
M-2	Catch ~ Year + Station, offset = log(Hooks)	32	33508	99201.72	317.68	99311.17	149.28	0.00	< 0.0001
M-3	$Catch \sim Year + Station + HPBC + CTNO, offset = log(Hooks)$	38	33505	99007.78	123.74	99167.75	5.86	0.00	< 0.0001
M-4	Catch ~ Year + Station + HPBC + Quarter + CTNO + Year:HPBC, offset = log(Hooks)	46	33501	98949.59	65.55	99176.92	15.03	0.00	< 0.0001
M-5	Catch ~ Year + Station + HPBC + Quarter + CTNO + Year:HPBC + HPBC:Quarter, offset = log(Hooks)	52	33498	98884.04	0.00	99161.89	0.00	1.00	< 0.0001

Table 3. Summary of yearly trends in blue shark CPUE in the Indian Ocean: relative nominal and standardized estimates from sdmTMB models, along with 95% CIs and CV for the best-fitting model.

Year	Relative nominal CPUE	Standardized CPUE (95%CIs)	CV
2005	0.395	0.452 (0.296 - 0.671)	0.280
2006	0.580	$0.562 \ (0.368 - 0.830)$	0.301
2007	0.716	$0.738 \ (0.488 - 1.067)$	0.298
2008	0.617	0.666 (0.420 - 1.000)	0.335
2009	1.525	1.421 (1.062 - 1.859)	0.213
2010	0.689	0.718 (0.527 - 0.952)	0.185
2011	1.053	$0.902 \ (0.642 - 1.230)$	0.271
2012	1.722	1.428 (1.163 - 1.751)	0.221
2013	1.929	1.745 (1.410 - 2.125)	0.120
2014	1.155	1.098 (0.827 - 1.413)	0.152
2015	0.486	0.563 (0.354 - 0.837)	0.217
2016	0.807	0.849 (0.581 - 1.181)	0.198
2017	1.042	1.012(0.764 - 1.305)	0.153
2018	1.017	$1.091 \ (0.807 - 1.435)$	0.175
2019	0.831	0.816 (0.593 - 1.099)	0.215
2020	0.634	0.727 (0.513 - 0.988)	0.208
2021	0.745	$0.786 \ (0.555 - 1.070)$	0.231
2022	1.711	1.406 (1.078 - 1.795)	0.177
2023	1.346	1.352 (1.044 -1.716)	0.170